Cancer Research

# Cancer Cell Dissemination and Homing to the Bone Marrow in a Zebrafish Model

Antonio Sacco[1], Aldo M. Roccaro[1,2], Dongdong Ma[3], Jiantao Shi[1], Yuji Mishima[1], Michele Moschetta[1], Marco Chiarini[1,2], Nikhil Munshi[1], Robert I. Handin[2], and Irene M. Ghobrial[1]

## Abstract

Advancement of many solid tumors and hematologic malignancies is frequently characterized by dissemination and homing of cancer cells to the bone marrow (BM). Methods to quantitatively characterize these key steps of the metastatic cascade in mammalian models are currently limited and do not offer opportunities to perform rapid, large-scale genomic, or drug screening. Because of their optical clarity, we used zebrafish to develop an *in vivo* model of cancer cell dissemination and homing to the BM. We performed intracardiac injection of multiple myeloma (MM) cells derived from human BM or cell lines and monitored their migration to the caudal hematopoietic tissue (CHT), the region where hematopoiesis occurs in the zebrafish embryo, which recapitulates a BM-like niche. Transcriptomic analyses confirmed that MM cells homing to the CHT displayed gene-expression differences compared with MM cells outside of the CHT, including significant enrichment for genes known to regulate interleukin-6 (IL6) signaling, cell adhesion, and angiogenesis. Collectively, our findings point to the zebrafish as a valuable model in which to study cancer cell homing to the hematopoietic niche and to establish a screening platform for the identification of factors and mechanisms contributing to the early steps of bone metastasis. *Cancer Res; 76(2); 463–71. ©2016 AACR.*

## Introduction

Cell metastasis is a multistep process that involves several steps, including cell invasion, egress, passage into the circulation, and specific homing to predetermined distant tissues. The bone marrow (BM) is one of the most critical organs for cell dissemination and cell metastasis in solid tumors such as prostate, breast and lung cancers, and in hematologic cancers, including multiple myeloma (MM) and leukemia. A similar process occurs with cell trafficking of hematopoietic stem cells (HSC) in and out of the BM. MM represents a good model to examine homing to the BM as it presents with multiple lesions in the BM by the time patients present with their disease (1, 2). The interaction between tumor cells and the surrounding BM microenvironment is essential for MM cell proliferation and dissemination, leading to disease progression and chemoresistance (1–12). For instance, the neutralization of CXCL12 within the BM niche reduces MM cell dissemination within the BM, leading to inhibition of MM disease progression (13). Thus, elucidating the mechanism of MM cell homing to the BM is essential to better define the pathogenesis of this disease and may be used to identify new therapeutic targets. Therefore, there is a real need to develop new modalities to assess MM tumor cell dissemination and homing to the BM.

To date, intravital two-photon and confocal microscopy have been used to visualize cancer cells within murine BM by exposing the BM within the calvarium of anesthetized animals (14). With this technique, it is possible to visualize cancer cells that home to the BM and establish contact with osteoblasts or the vasculature (1, 2, 10, 14–16). However, this technique is invasive and has limitations: (i) it is not quantitative; (ii) it cannot be used to analyze for screening studies such as drug screens or functional genomic studies such as shRNA or CRISPR screens; and (iii) it does not allow the use of primary cancer cells, as it requires a large number of tumor cells to be injected i.v. into the recipient mouse. In addition, many cells are trapped in the pulmonary vasculature and, therefore, precise quantification of the number of tumor cells reaching the BM and the assessment of any molecular alterations in MM cells is not possible.

There is recent evidence that many cytokines and chemokines are similar between zebrafish and that of mammals such as CXCL12, and that the hematopoietic role of the CXCR4–CXCL12 axis in zebrafish mirrors the functional role of CXCR4–CXCL12 in mammals (17). We therefore sought to develop a zebrafish model for assessment of tumor cell homing and metastasis to the BM by injecting either MM cell lines or patient-derived MM cells into zebrafish embryos and demonstrating their homing to the caudal hematopoietic tissue (CHT) where the HSCs migrate after their emergence from the ventral wall of the dorsal aorta: (18) This

[1]Department of Medical Oncology, Dana-Farber Cancer Institute, Harvard Medical School, Boston, Massachusetts. [2]Spedali Civili di Brescia, Centro per la Ricerca Onco-ematologica AIL, (CREA), Brescia, Italy. [3]Division of Hematology, Brigham and Women's Hospital, Harvard Medical School, Boston, Massachusetts.

**Note:** Supplementary data for this article are available at Cancer Research Online (http://cancerres.aacrjournals.org/).

A. Sacco and A.M. Roccaro share co-first authorship for this article.

R.I. Handin and I.M. Ghobrial share co-senior authorship for this article.

**Corresponding Authors:** Irene M. Ghobrial, Dana-Farber Cancer Institute, 450 Brookline Avenue, Boston, MA 02115. Phone: 617-632-4198; Fax: 617-582-8606; E-mail: irene_ghobrial@dfci.harvard.edu; and Robert I. Handin, Brigham and Women's Hospital, Harvard Medical School, Fifth Floor, Karp Family Research Building, One Blackfan Circle, Phone: 617-355-9066; Fax: 617-355-9124, rhandin@partners.org

**doi:** 10.1158/0008-5472.CAN-15-1926

posterior/caudal area is considered an early site of definitive hematopoiesis analogous to the mammalian fetal liver (19).

This model requires a very low number of MM cells to be injected (400 cells/embryo). We have demonstrated that the injected MM cells home to the BM-like CHT niche. Importantly, by performing RNA sequencing studies, we confirmed that those MM cells homing to the CHT present with specific changes in their transcriptome level that enables them for tropism to the BM. This accurately reflects the molecular alterations that are essential for MM cell homing to the BM niche. We propose this as a new model for studying mechanisms of cancer cell tropism to the BM. This can be used in screening studies to identify novel regulators of homing of cancer cells.

## Materials and Methods

### Patient samples, cell lines, and reagents

Tumor cell lines (MM.1S; MM.1S/GFP$^+$; BCWM.1; HeLa; MDA-MB-231) as well as primary human myeloma (MM) cells were used in these experiments. CD138$^+$ MM cells were derived from the BM of patients with MM ($n = 7$) by adsorption and elution from CD138-microbeads (Miltenyi Biotech), as previously described (2, 13). Approval for these studies was obtained from the Dana-Farber Cancer Institute Institutional Review Board. Informed consent was obtained from all patients and healthy volunteers in accordance with the Declaration of Helsinki protocol. Plerixafor was purchased from Selleckchem.

### Gain- and loss-of-function studies

*CXCR4*, *VLA4* and *FAK* genes were silenced in MM.1S cells with lentiviral shRNAs obtained from The RNAi Consortium (Broad Institute), as previously described (20). In addition, *CXCR4* was both silenced in BCWM.1, using shRNAs and lentivirus-mediated infection and overexpressed using either precision LentiORF/*CXCR4* (*CXCR4*$^+$) or empty vector (Thermo Fisher Scientific). The efficacy of gene-silencing or gain-of-function studies was evaluated by qRT-PCR as previously described (2).

### Zebrafish embryo homing model

All zebrafish experiments were performed as approved by the Harvard Medical Area Standing Committee on Animals. Embryos from the Casper (albino) strain of the zebrafish, *Danio Rerio*, were collected, staged, and raised at 28.5°C, according to standard experimental conditions. Embryos at 48 hours post-fertilization (hpf) were anesthetized using 0.04 mg/mL of tricaine (Sigma-Aldrich), placed onto a modified agarose gel mold for tumor cell microinjection. The tumor cell suspension was transferred using a micro-loader tip (Eppendorf) into a pre-pulled borosilicate glass needle (outer diameter/inner diameter: 1/0.5 mm; Sutter Instrument) connected to a Pico-Injector Microinjection Systems (PLI-100A; Harvard Apparatus, Harvard Biosciences, Inc.). Subsequent injection was conducted under a stereo-dissecting microscope (Leica, MZ75), via direct cardiac puncture as previously reported (21–23).

### Tumor cell labeling

Before injection, tumor cell lines (MM.1S, BCWM.1) and CD138$^+$ primary MM cells were labeled *in vitro* using the DiD or DiO vibrant cell labeling solution (Life Technologies), at a final concentration of 1 μmol/L in 0.1% BSA in RPMI-1640 for 30 minutes at 37°C in a 5% $CO_2$ atmosphere, as previously reported (16). In addition, GFP$^+$ MM.1S were also tested. About 400 of the labeled cells or GFP$^+$ cells were injected in each embryo. In some experiments, a mixture of cells labeled with either DiD (200 cells) or DiO (200 cells) in a total volume of 2 nL were injected. For each of the intracardiac injections, a total of 150 embryos were processed, with successful injection coupled with MM cell homing to the CHT occurring in of 70.6 (±10.3 SD) of the injected embryos.

### Zebrafish fluorescence activated cell sorting

CD41-GFP$^{low}$ zebrafish HSCs were flow-sorted from pooled single cell suspensions of dissected kidneys from Tg(CD41:GFP) fish, as previously described (18). Cell sorting was performed at the HSCI-BIDMC Flow Cytometry Core Facility.

### Quantification of migrated cells

Corrected total fluorescence (CTCF) was calculated using ImageJ software. The following formula was used to calculate the CTCF: CTCF = Integrated Density − (area of selected cell × mean fluorescence of background readings), as previously reported (24, 25).

### RNA extraction and RNA sequencing

RNA was isolated using an RNeasy kit (Qiagen). Poly-A selection and cDNA synthesis were performed, followed by library preparation using the Illumina TruSeq RNA Sample Preparation Kit (Illumina). Because the original sample is a mixture of human and zebrafish RNA, we used the Agilent SureSelect Human All Exon V5 Plus Kit to enrich human sequences. Libraries were sequenced on an Illumina Miseq with 75-bp paired-end reads. Bcbio_nextgen pipeline (https://github.com/chapmanb/bcbio-nextgen/) were used to process the RNA-seq data. Briefly, cutadapt (https://github.com/marcelm/cutadapt/) was used to trim adapters and trimmed reads were aligned to a Human reference genome (*GRCh37*) with TopHat2 (26). The read count for each gene was calculated by HT-seq (27). Normalized gene expression was expressed as fragments per kilobase of exon per million fragments mapped (FPKM), and estimated by Cufflinks2 (28). Data quality was assessed by RNA-SeQC (29).

## Results

### Homing of MM cells to the zebrafish CHT

We injected GFP$^+$MM.1S cells into zebrafish embryos 48 hpf (Fig. 1A), and assessed the ability of MM cells to enter the peripheral circulation and then traced their homing to the trunk region of zebrafish embryos—an area referred to as the CHT. HSCs are known to migrate to CHT (18), which is thought to be analogous to the mammalian fetal liver and is the area of definitive hematopoiesis in embryonic/fetal life (19). This and other observations suggest that zebrafish and mammalian hematopoiesis are comparable with similar cell lineages and, most importantly, crucial genetic modulators have been conserved through 200 million years of independent evolution (30).

Intravital confocal microscopy revealed the localization of GFP$^+$MM.1S cells within the CHT area. Uninjected zebrafish emhryos were used as controls (Fig. 1B). We next performed intracardiac injection of primary MM patient BM-derived CD138$^+$ cells that had been stained with either DiO or DiD and demonstrated that primary MM cells also homed to CHT (Fig. 1C). We also confirmed that DiO or DiD labeling did not affect the migratory ability of MM cells. We injected DiD-labeled MM.1S

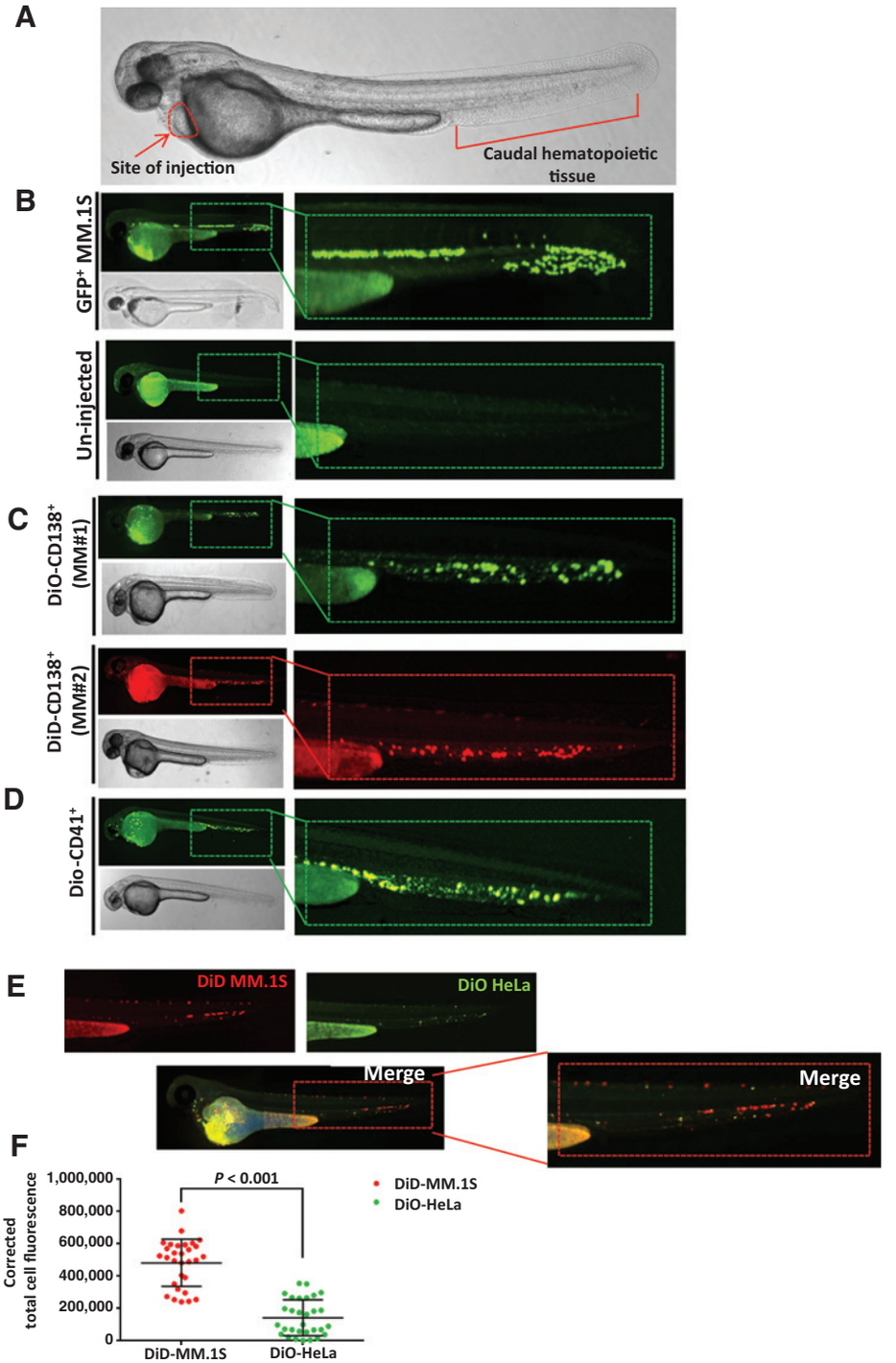


**Figure 1.**
Intracardiac injection of MM cells and their localization within the CHT-area. A, schematic representation of the site of intracardiac injection. B, $GFP^+$ MM.1S cells were injected intracardiac into zebrafish embryos 48 hpf. Visualization of MM cells at 30 minutes post-injection is depicted. Uninjected zebrafish embryos were used as a control. C, Primary $CD138^+$ cells were obtained from the BM of patients with active MM ($n = 7$) and labeled with either DiO or DiD and subsequently injected into zebrafish embryos 48 hpf. Visualization of MM cells obtained from two representative MM patients is shown. D, DiO-$CD41^+$-labeled zebrafish-derived $CD41^+$ cells were injected into zebrafish embryos 48 hpf, and used as a positive control, showing their colonization within the CHT niche, in a similar fashion to MM cells. E, DiD-labeled MM.1S and DiO-labeled HeLa cells were mixed in equal amount and subsequently injected into zebrafish embryos 48 hpf; only MM.1S cells homed to the CHT niche. F, quantification of the DiD/MM.1S and DiO/HeLa cells within the CHT niche was performed by measuring the corrected total fluorescence using ImageJ software.

cells mixed, in equal number, with DiO-labeled MM.1S cells, with equal distribution within the CHT niche (Supplementary Fig. S1).

To further validate that MM cells actually homed to the CHT, we injected DiO-labeled CD41-$GFP^{low}$ zebrafish HSCs that are known to home to the CHT hematopoietic niche. We observed that zebrafish-derived CD41-HSCs homed to the same area as the injected MM cells (Fig. 1D). To confirm that this phenomenon was restricted to MM cells, we injected DiD-labeled MM.1S cells mixed, in equal number, with DiO-HeLa cells, and demonstrated that the CHT area was colonized by MM cells but not by HeLa cells ($P < 0.001$; Fig. 1E and F).

We have further investigated whether other bone-metastasizing tumor cell lines, such as breast cancer cell lines, would home to the CHT niches, and found that intracardiac injection of MDA-MB-231 led to their colonization of the CHT areas (Supplementary Fig. S2). This indicates that MM cells, which

are known to home to the murine BM (2, 16, 31, 32), have the ability to migrate to the zebrafish CHT, similarly to other bone-tropic tumor cells, whereas other cancer cells that do not home to the BM were not able to home to CHT. These findings recapitulate the BM homing process that has been previously observed in mice (2, 16, 31, 32) and that occurs in patients with MM.

### RNA sequencing for studying MM cells interacting with the CHT niches

We next investigated whether this model could be used to analyze changes in the transcriptome of MM cells that have homed to the CHT-niche. We performed intracardiac injection of injected GFP$^+$/MM.1S cells, and selected only those zebrafish where MM cell homing to the CHT could be documented by fluorescence microscopy. A total of 60 zebrafish were selected. We carefully dissected the zebrafish embryos to separate the CHT from other tissue containing circulating nonadherent MM cells. For these experiments, 20 zebrafish were pooled into three separate pooled CHT and three pooled non-CHT samples and RNA isolated from each of the six pooled samples (Fig. 2A). Given the low number of human MM cells that homed to the CHT, we anticipated a low amount of human transcripts, so we performed whole human exome enrichment before sequencing of total RNA, as previously reported (33). This approach led to an alignment rate of 10% to 15%, with a high intragenic rate and exonic rate (> 95%) and low mismatch rate (~0.5%) for all the samples (Supplementary Table S1).

It is well accepted that MM cells depend on the surrounding BM microenvironment. For example, crucial factors that support the clonal expansion of MM cells, are, among others, the release of cytokines and chemokines that activate autocrine and paracrine circuits of growth, the adhesion of the MM cells to BM mesenchymal stromal cells, as well as the induction of neoangiogenesis (2, 3, 7, 8, 12, 20, 34–36). We therefore determined the gene-expression patterns of MM cells that homed to the CHT-niche and compared them with MM cells that did not home to the CHT. MM cells within the CHT had a significant enrichment of genes related to cytokine/chemokine–mediated signaling, IL6 pathway, cell–cell adhesion, and angiogenesis, as shown by GSEA (FDR < 0.25; $P < 0.05$; Fig. 2B). Overall, these findings indicate that the changes observed in MM cells that have homed to the CHT mirror those that are seen in MM cells in the human BM microenvironment (2, 3, 7, 8, 12, 20, 34–36).

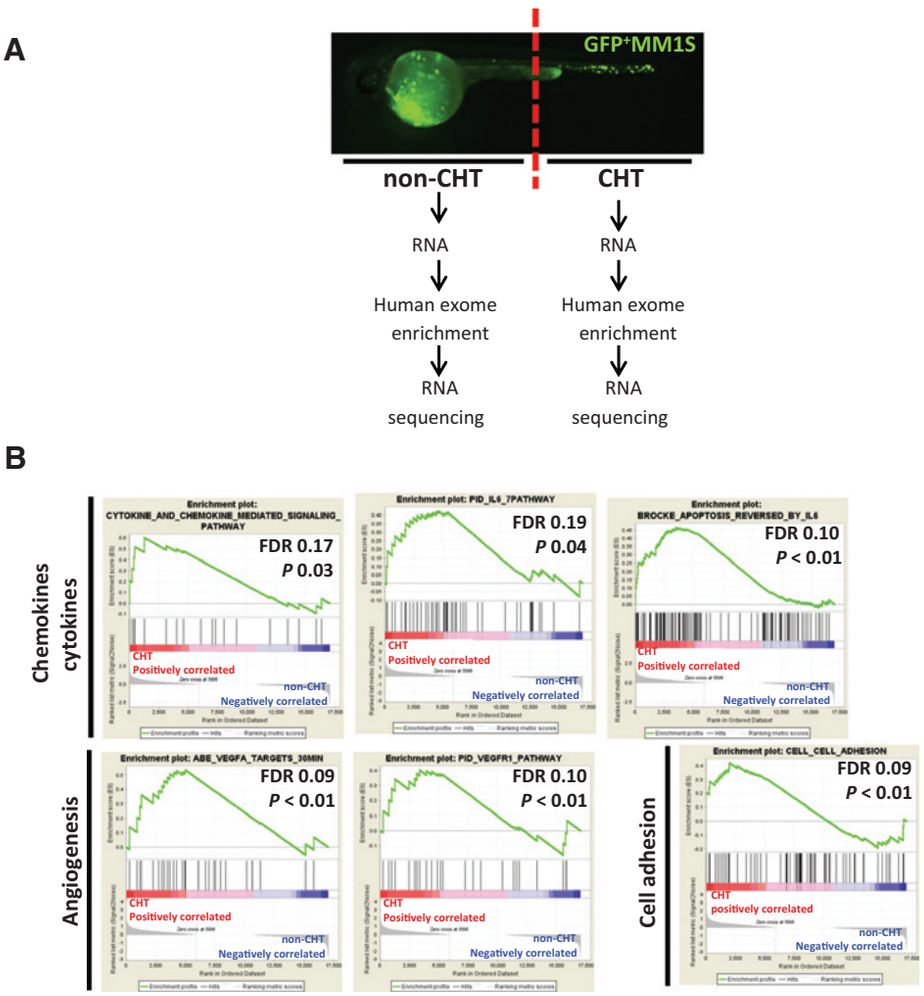


**Figure 2.**
RNA sequencing confirms specific changes at the transcriptome level in MM cells that homed to the CHT niches. A and B, GFP$^+$ MM.1S cells were injected into zebrafish embryos (48 hpf): 60 zebrafish embryos that had GFP$^+$ MM.1S cells within the CHT area were selected. The CHT niches were dissected and separated from the remaining body of the zebrafish embryos, which contained GFP$^+$ MM.1S that did not home to the CHT. RNA was extracted from the CHT and non-CHT niches and human exome enrichment was performed. The enriched samples were processed for RNA sequencing. A significant enrichment for chemokine/cytokine-, angiogenesis-, and cell adhesion–related mRNA signatures was demonstrated (FDR < 0.25: $P < 0.05$).

**Functional relevance of the zebrafish model in the context of MM**

We next investigated whether zebrafish use the same molecular mechanisms for cell homing as mammals. It is well known that the CXCR4–CXCL12 axis plays a major role in supporting the migration and adhesion of MM cells in the BM niche (1, 16). Moreover, the homing of MM cells to the BM is also regulated by additional factors, such as the activation of VLA-4 (37), an integrin expressed on MM cells and known to promote their migration to the BM niche (38). Other factors to be taken into consideration as modulators of the homing of tumor cells to the BM, include focal adhesion kinase (FAK) that enhances the localization and retention of B-lineage cells within the BM niche (39).

To investigate the functional relevance of the zebrafish model, we established *CXCR4*, *VLA4* and *FAK*-silenced MM cells and compared their ability to home to CHT with that of control cells infected with a scrambled shRNA. The efficacy of silencing for each specific target was evaluated by qRT-PCR ($P< 0.05$; Supplementary Fig. S3A–S3C). DiO-labeled-*CXCR4*-silenced and DiO-labeled-scrambled-probe–infected MM cells were mixed in equal numbers and subsequently injected into recipient zebrafish. We found a significant reduction in the number of *CXCR4*-silenced MM cells homing to the CHT, compared with the control cells ($P < 0.001$; Fig. 3A). To further corroborate the *CXCR4*-dependent modulation of MM cell homing to CHT, we treated MM.1S cells with AMD-3100 (Plerixafor) and confirmed that Plerixafor-mediated inhibition of CXCR4 also inhibited the homing of MM cells as compared with vehicle-treated control cells ($P < 0.001$; Fig. 3B). We then examined *VLA4*- and *FAK*–knockdown MM cells and observed that the homing of MM cells to CHT was impaired when either *VLA4* or *FAK* cells were silenced ($P < 0.001$; Fig. 3C and D). All together, these findings, therefore, confirm that the proposed zebrafish model is functionally relevant to the biology of MM.

As a proof of concept, due to the demonstrated functional importance of *CXCR4*, *VLA4* and *FAK* in mediating MM cell homing to the CHT niches, we next performed qRT-PCR for those selected genes, and confirmed that MM cells harvested from the CHT areas expressed higher levels of *CXCR4*, *VLA4* and *FAK*, compared with MM cells harvested from non-CHT areas, thus further confirming the functional relevance of this model ($P < 0.05$; Fig. 3E).

**Applicability and functional relevance of the zebrafish model in the context of another B-cell malignancy with specific tropism to the BM**

To further investigate whether tumor specific tropism to zebrafish embryo CHT is applicable to other hematologic malignancies that are known to home to the human and murine BM, we used a cultured cell lined derived from a patient with Waldenstrom's macroglobulinemia (WM; refs. 13, 37). We assessed the effect of gain and loss of *CXCR4* expression BCWM.1 cells of homing in zebrafish embryos. The efficacy of *CXCR4* silencing and overexpression was evaluated by qRT-PCR ($P < 0.05$; Supplementary Fig. S3D and S3E). We then injected either *CXCR4*-overexpressing or *CXCR4*-silenced WM cells and found that increased *CXCR4* expression in WM cells led to enhanced CHT-homing of WM cells ($P<0.001$; Fig. 4A), whereas the homing of *CXCR4*-silenced WM cells to the CHT was reduced when compared with scrambled control ($P<0.001$; Fig. 4B).

## Discussion

The mechanisms by which MM cells and many other metastatic tumors preferentially home to the BM are not well understood. Bone metastasis represented nearly 70% of cases of metastasis in breast and prostate cancer and approximately 15% of other carcinomas such as lung, colon, and renal cell carcinoma. Most hematologic malignancies preferentially traffic to the BM. However, many of the factors that contribute to the selective homing of cancer cells to the BM are not identified (1, 2, 16, 40). The MM plasma cell–BM interaction favors MM cell growth and leads to further dissemination and disease progression. It is, therefore, important to define the interaction between the cancer cells and the surrounding BM niche, to better understand those changes that occur during the early dissemination and homing of these cells. Here, we used MM as a model for BM dissemination and metastasis. We used cell lines and patient samples demonstrating that this model can be used for patient samples in a large screen to identify subclones that have the propensity for cell dissemination and metastasis to hematopoietic niches.

Previous reports have demonstrated the value of murine xenograft MM models, coupled with bioluminescent imaging (BLI) to monitor tumor growth (2, 16, 31, 41–43). This is a good approach for drug screens, but cannot be used for a large drug screen as it would require a large number of mice and it can be used to examine the effect of drugs on the early steps of homing and engraftment. Similarly, other imaging modalities using to examine homing such as intravital confocal microscopy that permits the visualization of cancer cells within the BM through the calvarial bones of the mouse skull have been useful (2, 10, 13–16, 32), but these techniques have limitations, including the lack of ability to quantify the number of cells that disseminate to the BM, loss of many of the injected cells by entrapment in lung tissue and an inability to scale this model for high-throughput screening with RNAi screen or drug screens. Moreover, repeated imaging of the same mouse is limited by the development of scar tissue, which may impair visualization of the BM.

To provide added resolution and flexibility, we therefore developed a novel model for the study of early MM cell homing, by injecting MM cells into zebrafish embryos. This allowed us to follow MM cell homing to a BM-like niche within a few minutes after MM cell injection, and allowed the visualization of the behavior of a very low number of tumor cells, as well as the ability to study patient-derived MM cells. One other advantage of this technique is that one can admix experimental (e.g., drug treated or gene silenced) and control cells and compare their early BM homing ability in the same animal. We have also shown here that it is also possible to make accurate estimates of cell number in the zebrafish. Thus, this technique complements the murine model, where the intravital confocal visualization of MM cells is possible, but only after the injection of a much larger number of MM cells.

In addition, we were able to harvest MM cells from recipient zebrafish for RNA sequencing and transcriptome analysis. The changes observed in the MM cells following interaction with the CHT-niche are identical to those that are usually seen after the interaction of MM cells with the human BM microenvironment (2, 3, 7, 8, 12, 20, 34–36). Indeed, enrichment for cytokine/chemokine-, angiogenesis-, cell–cell adhesion–related mRNA signatures was confirmed in MM cells that had homed to the CHT.

It could be envisioned that this technique can also be used in the future to identify at the single-cell level or subclonal level, cells

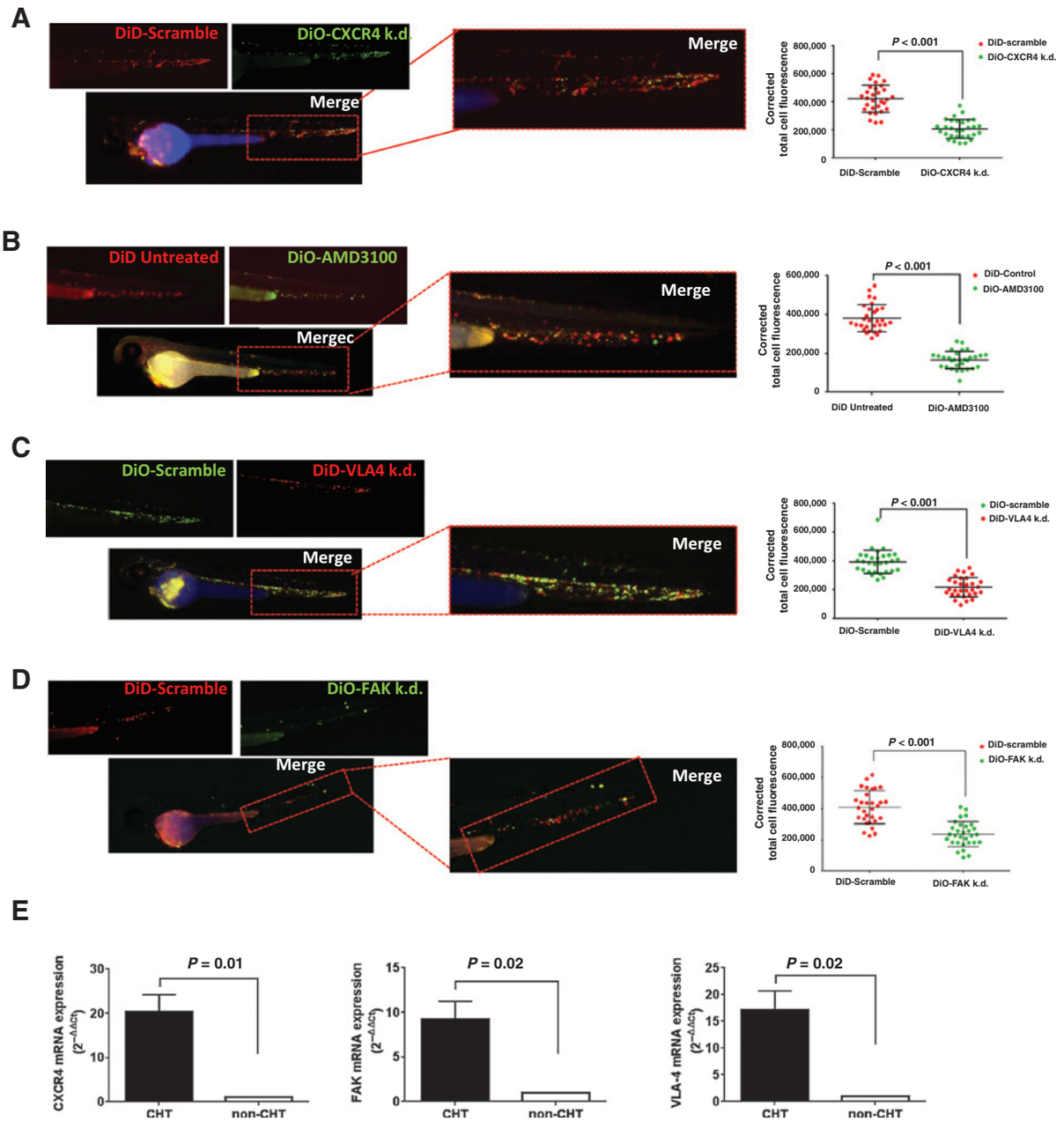


**Figure 3.**

*CXCR4, VLA4* and *FAK* silencing led to inhibited MM cell homing to the CHT-area. A, *CXCR4* k.d. and control scrambled MM.1S cells were labeled with DiO and DiD, respectively. The labeled cells were mixed in equal number and injected into recipient zebrafish embryos 48 hpf (zebrafish $n = 30$ in each group). Quantification of the DiD-labeled scrambled control- and DiO-*CXCR4* k.d cells within the CHT niche was performed by measuring the corrected total fluorescence using ImageJ software, showing significant reduction in CHT infiltration of DiO-*CXCR4* k.d. MM.1S cells compared with DiD-control cells. B, DiO-labeled MM.1S cells were treated with plerixafor (20 μmol/L) for 4 hours. Untreated DiD-labeled MM.1S cells were used as control. DiO- and DiD-labeled cells were mixed in equal number and injected into recipient zebrafish embryos 48 hpf (zebrafish *n*:30/each group). Quantification of the DiD-control cells and DiO-plerixafor–treated cells within the CHT niche was performed by measuring the corrected total fluorescence using ImageJ software, showing significant reduction in CHT-infiltration of DiO-plerixafor–treated MM.1S cells compared with DiD-control cells. C, scrambled control MM.1S cells were labeled with DiO and *VLA4* k.d. MM.1S cells were labeled with DiD. DiO- and DiD-labeled cells were mixed in equal number and injected into recipient zebrafish embryos 48 hpf (zebrafish $n = 30$ in each group). Quantification of the DiO-scrambled control and DiD-*VLA4* k.d cells within the CHT niche was performed by measuring the corrected total fluorescence using ImageJ software, showing significant reduction in CHT-infiltration of DiD-*VLA4* k.d. MM.1S cells compared with DiO-scrambled control cells. D, scrambled control MM.1S cells were labeled with DiD; *FAK* k.d. MM.1S cells were labeled with DiO. DiD- and DiO-labeled cells were mixed in equal number and injected in recipient zebrafish embryos 48 hpf (zebrafish $n = 30$ in each group). Quantification of the DiD-scrambled control and DiO-*FAK* k.d. cells within the CHT niche was performed by measuring the corrected total fluorescence using ImageJ software, showing significant reduction in CHT-infiltration of DiO-*FAK* k.d. MM.1S cells compared with DiD-scrambled control cells. E, modulation of specific targets (*CXCR4, VLA4* and *FAK*) was demonstrated using MM.1S cells harvested from the CHT niche compared with MM.1S cells that did not home to the CHT niche, by qRT-PCR.

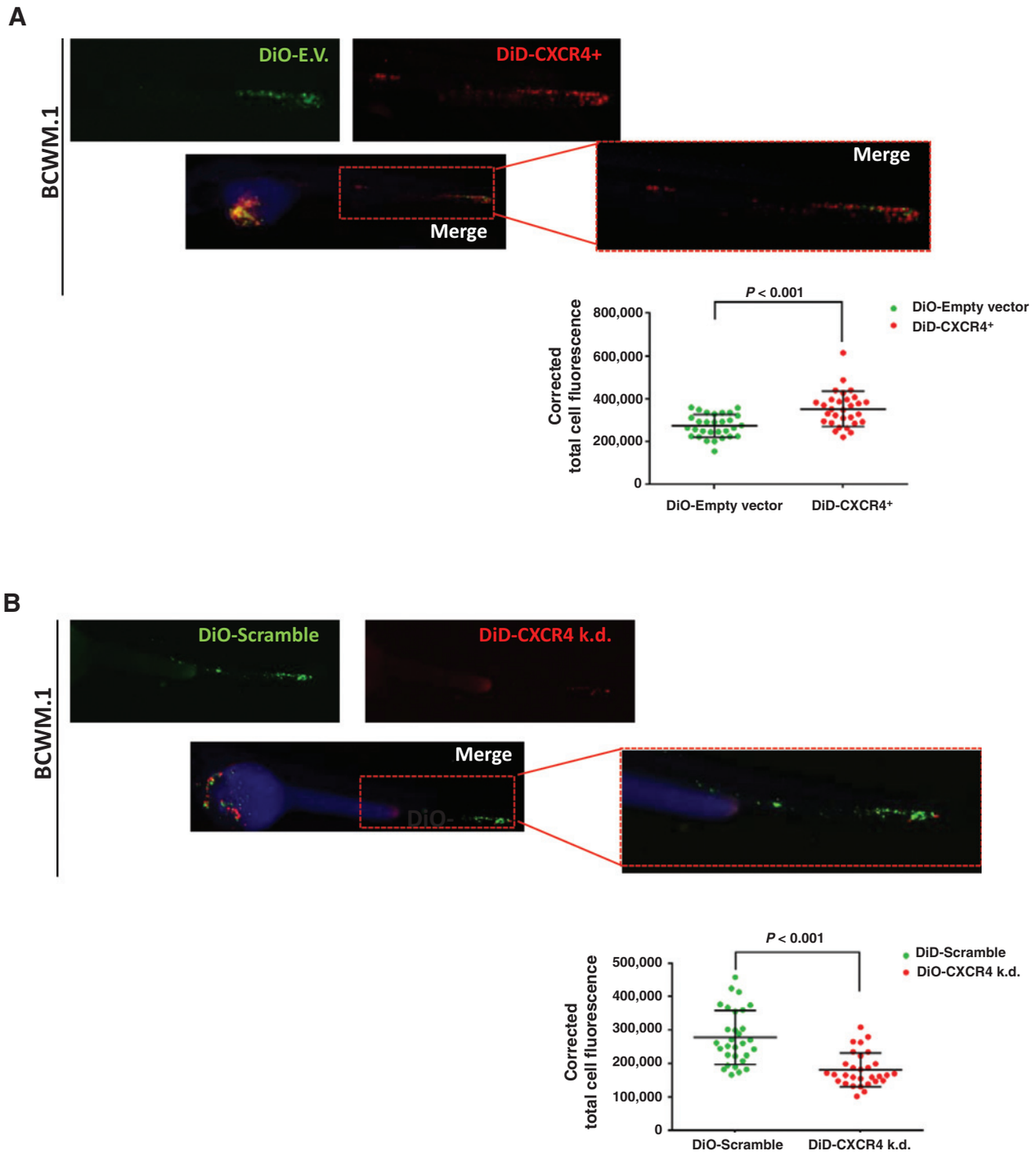


**Figure 4.**
*CXCR4* gain and loss of functions modulate WM cell homing to the CHT niche. Empty vector–infected BCWM.1 cells were labeled with DiO; *CXCR4* overexpressing cells (*CXCR4*$^+$) were labeled with DiD. DiO- and DiD-labeled cells were mixed in equal number and injected intracardiac in recipient zebrafish embryos 48 hpf (zebrafish *n*:30/each group). Quantification of the DiO–empty vector and DiD–*CXCR4*$^+$ cells within the CHT niches was performed by measuring the corrected total fluorescence using ImageJ software, showing enhanced CHT-infiltration of DiD-*CXCR4*$^+$ cells compared with DiO-empty vector control cells. B, scramble-infected BCWM.1 cells were labeled with DiO; *CXCR4* k.d. cells were labeled with DiD. DiO- and DiD-labeled cells were mixed in equal number and injected intracardiac in recipient zebrafish embryos 48 hpf (zebrafish *n*:30/each group). Quantification of the DiO-scramble and DiD-*CXCR4* k.d. cells within the CHT niches was performed by measuring the corrected total fluorescence using ImageJ software, showing inhibited CHT-infiltration of DiD-*CXCR4* k.d. cells compared with DiO–empty vector control cells.

that have the propensity for homing and metastasis within a larger tumor bulk or within primary tumor samples. Taken together, these observations provide compelling evidence that intra-cardiac injection of tumor cells into zebrafish embryos is a useful new technique for rapid screening of cancer cells that can home or metastasize to the BM. In future studies, this approach might be applied to the analysis of the dissemination and homing of other cancers to identify molecular factors that regulate early cell dissemination and homing to the hematopoietic niche.

## Disclosure of Potential Conflicts of Interest

N. Munshi has ownership interest (including patents) in Oncopep and is a consultant/advisory board member for Celgene, Takeda, Merck, Pfizer, Oncopep. No potential conflicts of interest were disclosed by the other authors.

## Authors' Contributions

**Conception and design:** A. Sacco, A.M. Roccaro
**Development of methodology:** A. Sacco, A.M. Roccaro, D. Ma, M. Chiarini, N. Munshi, R.I. Handin
**Acquisition of data (provided animals, acquired and managed patients, provided facilities, etc.):** A. Sacco, A.M. Roccaro, D. Ma, M. Moschetta, R.I. Handin
**Analysis and interpretation of data (e.g., statistical analysis, biostatistics, computational analysis):** A. Sacco, A.M. Roccaro, J. Shi, Y. Mishima. R.I. Handin
**Writing, review, and/or revision of the manuscript:** A. Sacco, A.M. Roccaro, D. Ma, N. Munshi, R.I. Handin, I.M. Ghobrial
**Administrative, technical, or material support (i.e., reporting or organizing data, constructing databases):** Y. Mishima. R.I. Handin
**Study supervision:** A.M. Roccaro, R.I. Handin, I.M. Ghobrial

## Acknowledgments

The Leukemia and Lymphoma Society New Idea Award.

The costs of publication of this article were defrayed in part by the payment of page charges. This article must therefore be hereby marked *advertisement* in accordance with 18 U.S.C. Section 1734 solely to indicate this fact.

Received July 16, 2015; revised October 1, 2015; accepted October 19, 2015; published OnlineFirst January 7, 2016.

## References

1. Alsayed Y, Ngo H, Runnels J, Leleu X, Singha UK, Pitsillides CM, et al. Mechanisms of regulation of CXCR4/SDF-1 (CXCL12)-dependent migration and homing in multiple myeloma. Blood 2007;109:2708–17.
2. Roccaro AM, Sacco A, Purschke WG, Moschetta M, Buchner K, Maasch C, et al. SDF-1 inhibition targets the bone marrow niche for cancer therapy. Cell Rep 2014;9:118–28.
3. Anderson KC, Lust JA. Role of cytokines in multiple myeloma. Semin Hematol 1999;36(1 Suppl 3):14–20.
4. Basak GW, Srivastava AS, Malhotra R, Carrier E. Multiple myeloma bone marrow niche. Curr Pharm Biotechnol 2009;10:345–6.
5. Basile A, Moschetta M, Ditonno P, Ria R, Marech I, De Luisi A, et al. Pentraxin 3 (PTX3) inhibits plasma cell/stromal cell cross-talk in the bone marrow of multiple myeloma patients. J Pathol 2013;229:87–98.
6. Cheung WC, Van Ness B. The bone marrow stromal microenvironment influences myeloma therapeutic response *in vitro*. Leukemia 2001;15:264–71.
7. Frassanito MA, Rao L, Moschetta M, Ria R, Di Marzo L, De Luisi A, et al. Bone marrow fibroblasts parallel multiple myeloma progression in patients and mice: *in vitro* and *in vivo* studies. Leukemia 2014;28:904–16.
8. Hideshima T, Mitsiades C, Tonon G, Richardson PG, Anderson KC. Understanding multiple myeloma pathogenesis in the bone marrow to identify new therapeutic targets. Nat Rev Cancer 2007;7:585–98.
9. Meads MB, Hazlehurst LA, Dalton WS. The bone marrow microenvironment as a tumor sanctuary and contributor to drug resistance. Clin Cancer Res 2008;14:2519–26.
10. Roccaro AM, Sacco A, Maiso P, Azab AK, Tai YT, Reagan M, et al. BM mesenchymal stromal cell-derived exosomes facilitate multiple myeloma progression. J Clin Invest 2013;123:1542–55.
11. Vacca A, Ria R, Ribatti D, Semeraro F, Djonov V, Di Raimondo F, et al. A paracrine loop in the vascular endothelial growth factor pathway triggers tumor angiogenesis and growth in multiple myeloma. Haematologica 2003;88:176–85.
12. Vacca A, Ria R, Semeraro F, Merchionne F, Coluccia M, Boccarelli A, et al. Endothelial cells in the bone marrow of patients with multiple myeloma. Blood 2003;102:3340–8.
13. Roccaro AM, Sacco A, Jimenez C, Maiso P, Moschetta M, Mishima Y, et al. C1013G/CXCR4 acts as a driver mutation of tumor progression and modulator of drug resistance in lymphoplasmacytic lymphoma. Blood 2014;123:4120–31.
14. Runnels JM, Carlson AL, Pitsillides C, Thompson B, Wu J, Spencer JA, et al. Optical techniques for tracking multiple myeloma engraftment, growth, and response to therapy. J Biomed Opt 2011;16:011006.
15. Azab AK, Hu J, Quang P, Azab F, Pitsillides C, Awwad R, et al. Hypoxia promotes dissemination of multiple myeloma through acquisition of epithelial to mesenchymal transition-like features. Blood 2012;119:5782–94.
16. Azab AK, Runnels JM, Pitsillides C, Moreau AS, Azab F, Leleu X, et al. CXCR4 inhibitor AMD3100 disrupts the interaction of multiple myeloma cells with the bone marrow microenvironment and enhances their sensitivity to therapy. Blood 2009;113:4341–51.
17. Glass TJ, Lund TC, Patrinostro X, Tolar J, Bowman TV, Zon LI, et al. Stromal cell-derived factor-1 and hematopoietic cell homing in an adult zebrafish model of hematopoietic cell transplantation. Blood 2011;118:766–74.
18. Ma D, Zhang J, Lin HF, Italiano J, Handin RI. The identification and characterization of zebrafish hematopoietic stem cells. Blood 2011;118:289–97.
19. Murayama E, Kissa K, Zapata A, Mordelet E, Briolat V, Lin HF, et al. Tracing hematopoietic precursor migration to successive hematopoietic organs during zebrafish development. Immunity 2006;25:963–75.
20. Zhang Y, Moschetta M, Huynh D, Tai YT, Zhang Y, Zhang W, et al. Pyk2 promotes tumor progression in multiple myeloma. Blood 2014;124:2675–86.
21. de Jong JL, Burns CE, Chen AT, Pugach E, Mayhall EA, Smith AC, et al. Characterization of immune-matched hematopoietic transplantation in zebrafish. Blood 2011;117:4234–42.
22. Hoffman SJ, Psaltis PJ, Clark KJ, Spoon DB, Chue CD, Ekker SC, et al. An *in vivo* method to quantify lymphangiogenesis in zebrafish. PloS ONE 2012;7:e45240.
23. LeBlanc J, Bowman TV, Zon L. Transplantation of whole kidney marrow in adult zebrafish. J Vis Exp 2007;2:159.
24. Cappell KM, Sinnott R, Taus P, Maxfield K, Scarbrough M, Whitehurst AW. Multiple cancer testis antigens function to support tumor cell mitotic fidelity. Mol Cell Biol 2012;32:4131–40.
25. Rahman MM, Rosu S, Joseph-Strauss D, Cohen-Fix O. Down-regulation of tricarboxylic acid (TCA) cycle genes blocks progression through the first mitotic division in Caenorhabditis elegans embryos. Proc Natl Acad Sci U S A 2014;111:2602–7.
26. Kim D, Pertea G, Trapnell C, Pimentel H, Kelley R, Salzberg SL. TopHat2: accurate alignment of transcriptomes in the presence of insertions, deletions, and gene fusions. Genome Biol 2013;14:R36.
27. Anders S, Pyl PT, Huber W. HTSeq—a Python framework to work with high-throughput sequencing data. Bioinformatics 2015;31:166–9.
28. Trapnell C, Williams BA, Pertea G, Mortazavi A, Kwan G, van Baren MJ, et al. Transcript assembly and quantification by RNA-Seq reveals unannotated transcripts and isoform switching during cell differentiation. Nat Biotechnol 2010;28:511–5.

29. DeLuca DS, Levin JZ, Sivachenko A, Fennell T, Nazaire MD, Williams C, et al. RNA-SeQC: RNA-seq metrics for quality control and process optimization. Bioinformatics 2012;28:1530–2.
30. Bertrand JY, Traver D. Hematopoietic cell development in the zebrafish embryo. Curr Opin Hematol 2009;16:243–8.
31. Azab AK, Azab F, Blotta S, Pitsillides CM, Thompson B, Runnels JM, et al. RhoA and Rac1 GTPases play major and differential roles in stromal cell-derived factor-1–induced cell adhesion and chemotaxis in multiple myeloma. Blood 2009;114:619–29.
32. Roccaro AM, Sacco A, Thompson B, Leleu X, Azab AK, Azab F, et al. MicroRNAs 15a and 16 regulate tumor proliferation in multiple myeloma. Blood 2009;113:6669–80.
33. Halvardson J, Zaghlool A, Feuk L. Exome RNA sequencing reveals rare and novel alternative transcripts. Nucleic Acids Res 2013;41:e6.
34. Bataille R, Jourdan M, Zhang XG, Klein B. Serum levels of interleukin 6, a potent myeloma cell growth factor, as a reflect of disease severity in plasma cell dyscrasias. J Clin Invest 1989;84:2008–11.
35. Zhang XG, Klein B, Bataille R. Interleukin-6 is a potent myeloma-cell growth factor in patients with aggressive multiple myeloma. Blood 1989;74:11–3.
36. Vacca A, Ribatti D. Bone marrow angiogenesis in multiple myeloma. Leukemia 2006;20:193–9.
37. Ngo HT, Leleu X, Lee J, Jia X, Melhem M, Runnels J, et al. SDF-1/CXCR4 and VLA-4 interaction regulates homing in Waldenstrom macroglobulinemia. Blood 2008;112:150–8.
38. Sanz-Rodriguez F, Ruiz-Velasco N, Pascual-Salcedo D, Teixido J. Characterization of VLA-4–dependent myeloma cell adhesion to fibronectin and VCAM-1. Br J Haematol 1999;107:825–34.
39. Park SY, Wolfram P, Canty K, Harley B, Nombela-Arrieta C, Pivarnik G, et al. Focal adhesion kinase regulates the localization and retention of pro-B cells in bone marrow microenvironments. J Immunol 2013;190:1094–102.
40. Roodman GD. Mechanisms of bone metastasis. Discov Med 2004;4:144–8.
41. Delmore JE, Issa GC, Lemieux ME, Rahl PB, Shi J, Jacobs HM, et al. BET bromodomain inhibition as a therapeutic strategy to target c-Myc. Cell 2011;146:904–17.
42. Labrinidis A, Diamond P, Martin S, Hay S, Liapis V, Zinonos I, et al. Apo2L/TRAIL inhibits tumor growth and bone destruction in a murine model of multiple myeloma. Clin Cancer Res 2009;15:1998–2009.
43. Rozemuller H, van der Spek E, Bogers-Boer LH, Zwart MC, Verweij V, Emmelot M, et al. A bioluminescence imaging based *in vivo* model for preclinical testing of novel cellular immunotherapy strategies to improve the graft-versus-myeloma effect. Haematologica 2008;93:1049–57.